

Disrupted brain anatomical connectivity in medication-naïve patients with first-episode schizophrenia

Ruibin Zhang · Qinling Wei · Zhuang Kang · Andrew Zalesky · Meng Li ·
Yong Xu · Leijun Li · Junjing Wang · Liangrong Zheng · Bin Wang ·
Jingping Zhao · Jinbei Zhang · Ruiwang Huang

Received: 22 June 2013 / Accepted: 4 January 2014 / Published online: 22 January 2014
© Springer-Verlag Berlin Heidelberg 2014

Abstract Previous studies suggested that the topological properties of brain anatomical networks may be aberrant in schizophrenia (SCZ), and most of them focused on the chronic and antipsychotic-medicated SCZ patients which may introduce various confounding factors due to antipsychotic medication and duration of illness. To avoid those potential confounders, a desirable approach is to select medication-naïve, first-episode schizophrenia (FE-SCZ) patients. In this study, we acquired diffusion tensor imaging datasets from 30 FE-SCZ patients and 34 age- and gender-matched healthy controls. Taking a distinct gray matter region as a node, inter-regional connectivity as edge and the corresponding streamline counts as edge weight, we constructed whole-brain anatomical networks for both groups, calculated their topological parameters using graph theory, and compared their between-group differences using non-parametric permutation tests. In addition, network-based statistic method was utilized to identify inter-regional

connections which were impaired in the FE-SCZ patients. We detected only significantly decreased inter-regional connections in the FE-SCZ patients compared to the controls. These connections were primarily located in the frontal, parietal, occipital, and subcortical regions. Although small-worldness was conserved in the FE-SCZ patients, we found that the network strength and global efficiency as well as the degree were significantly decreased, and shortest path length was significantly increased in the FE-SCZ patients compared to the controls. Most of the regions that showed significantly decreased nodal parameters belonged to the top-down control, sensorimotor, basal ganglia, and limbic-visual system systems. Correlation analysis indicated that the nodal efficiency in the sensorimotor system was negatively correlated with the severity of psychosis symptoms in the FE-SCZ patients. Our results suggest that the network organization is changed in the early stages of the SCZ disease process. Our findings provide useful information for further understanding the brain white matter dysconnectivity of schizophrenia.

R. Zhang and Q. Wei have contributed equally to this work.

Electronic supplementary material The online version of this article (doi:10.1007/s00429-014-0706-z) contains supplementary material, which is available to authorized users.

R. Zhang · M. Li · Y. Xu · J. Wang · B. Wang · R. Huang (✉)
Brain Imaging Center, Guangdong Key Laboratory of Mental Health and Cognitive Science, Center for the Study of Applied Psychology, School of Psychology, South China Normal University, Guangzhou 510631,
People's Republic of China
e-mail: ruiwang.huang@gmail.com

Q. Wei · L. Li · L. Zheng · J. Zhang (✉)
Department of Psychiatry, The Third Affiliated Hospital of Sun Yat-sen University, Guangzhou 510631,
People's Republic of China
e-mail: weiqi.yuelu@aliyun.com

Keywords Diffusion tensor imaging (DTI) · Tractography · Networks · Robustness · Dysconnectivity

Q. Wei · J. Zhao
Mental Health Institute, The Second Xiangya Hospital, Central South University, Changsha 410011, Hunan,
People's Republic of China

Z. Kang
Department of Radiology, The Third Affiliated Hospital of Sun Yat-sen University, Guangzhou 510631,
People's Republic of China

A. Zalesky
Melbourne Neuropsychiatry Centre, University of Melbourne and Melbourne Health, Melbourne, VIC, Australia

Introduction

Schizophrenia (SCZ) is a devastating illness characterized by a breakdown in thought processes and poor emotional responsiveness. Commonly observed symptoms include hallucinations, delusions, loss of initiative, disorganized speech and thinking, and cognitive deficits (Amador and Gorman 1998; Friston 1999). Previous studies suggested that SCZ may involve not only aberrant brain gray matter tissue but also “miswiring” between brain regions (Douaud et al. 2007; Beasley et al. 2009). Brain white matter (WM) connecting different regions into networks may be relevant to the pathophysiology of the psychosis syndrome and has become a major interest in SCZ research (Kunimatsu et al. 2012; Camchong et al. 2009; Schlösser et al. 2007).

Diffusion-weighted magnetic resonance imaging (DW-MRI) is the only available noninvasive technique for visualizing white matter trajectories in the human brain in vivo. Since Hagmann et al. (2007) adopted diffusion images and tractography to study human brain anatomical networks, the whole-brain approach has been increasingly applied to explore changes in human anatomical network properties in neuropsychiatric disorders (Wen et al. 2011; Xia and He 2011). Several studies (van den Heuvel et al. 2010; Zalesky et al. 2011; Wang et al. 2012) have reported alterations in the topological properties of whole-brain anatomical networks in SCZ patients. However, most of these studies focused on chronic and antipsychotic-medicated SCZ patients (Table S6 in Supplement), which may introduce various confounders due to antipsychotic medication (particularly medical conditions related to second-generation antipsychotics) or potential WM changes due to aging or illness duration. Previous studies indicated that illness duration may impact brain WM progressively (Friedman et al. 2008; Kong et al. 2011; Rosenberger et al. 2008) and antipsychotic medications may affect brain anatomy (Heitmiller et al. 2004; Navari and Dazzan 2009). Thus, to avoid those potential confounders and identify the naive topological organization of SCZ, an optimal approach is to select medication-naïve, first-episode schizophrenia (FE-SCZ) patients. However, very few studies have investigated topological properties of brain anatomical networks in FE-SCZ or in the early phase of medication-naïve SCZ patients.

Using diffusion tensor imaging (DTI), several studies have investigated brain WM microstructure alterations in FE-SCZ patients. Cheung et al. (2008, 2011) found a decreased fractional anisotropy (FA) in the left fronto-occipital fasciculus and left inferior longitudinal fasciculus and significantly negative correlation between the PASS positive score and the value of FA in the left fronto-occipital fasciculus and between the PASS positive score and the PASS positive score in the left inferior longitudinal fasciculus in FE-SCZ patients. Gasparotti et al. (2009)

found reduced FA values in the splenium of corpus callosum in FE-SCZ patients compared to the healthy controls. In addition, several studies (Filippi et al. 2013; Guo et al. 2012) detected aberrant FA values in the right superior longitudinal fasciculus, right fornix, right internal capsule, and right external capsule in FE-SCZ patients. Although these studies reflect that aberrant WM integrity may exist before the onset of schizophrenia, most of them have not directly investigated WM connectivity per se. Considering inter-regional “dysconnection” in SCZ has been proposed in a meta-analysis study (Ellison-Wright et al. 2008), a network model may be a more obvious method for detecting significantly altered fiber bundles in FE-SCZ patients.

With the aim to detect aberrant inter-regional white matter connections and to pinpoint alterations in the network organization, we recruited 30 FE-SCZ patients and 34 healthy controls in current study. Each pairs of nodes were linked if they are interconnected via sufficient streamline counts using DTI and whole-brain tractography. Network properties by the graph theory were investigated, enabling determination of whether the network organization was changed in FE-SCZ. Then a network-based statistic (NBS) method, to control the family-wise error rate when mass-univariate testing, was performed at every connection comprising the network to detect the impaired connections.

Methods and materials

Subjects

Thirty FE-SCZ patients (10 F/20 M, aged 18–45 years, mean \pm SD = 24.8 \pm 6.2 years) participated in this study. They were recruited from the Inpatient Units of the Department of Psychiatry, the third Affiliated Hospital of Sun Yat-sen University. These patients were free from the influence of antipsychotic medication and disentangled from the primary connectivity pathology of SCZ. All were right-handed and met the Diagnostic and Statistical Manual of Mental Disorders, Fourth Edition (DSM-IV) criteria. The DSM-IV diagnosis was made by an experienced psychiatrist (QW) using the patient version of the Structured Clinical Interview for DSM-IV (SCID-I/P). Their symptoms were all rated by the same psychiatrist (QW) using the Positive and Negative Syndrome Scale (PANSS) (von Knorring and Lindstrom 1992). And the patients who have persistent headaches or head trauma, electroconvulsive therapy, psychostimulant use, neuroleptic use, history of neurological problems, and special school attendance were excluded. In addition, we recruited 34 age-, gender-, and handedness-matched healthy subjects to serve as the healthy controls. The exclusion criteria for the controls were

Table 1 Demographic and clinical details of the medication-naïve, first-episode schizophrenia (FE-SCZ) patients and the healthy controls (HC) in this study

Characteristics	FE-SCZ (<i>n</i> = 30)	HC (<i>n</i> = 34)	<i>p</i> value
Male/female	20/10	22/12	0.87 ^a
Age: mean ± <i>SD</i> (years)	24.8 ± 6.16	25.3 ± 5.56	0.75 ^b
Level of education: mean ± <i>SD</i> (years)	12.3 ± 2.60	12.3 ± 2.64	0.99 ^b
Age episode: mean ± <i>SD</i> (years)	24.3 ± 6.25	<i>n.s.</i>	<i>n.s.</i>
Duration of illness untreated: median (weeks)	9	<i>n.s.</i>	<i>n.s.</i>
<i>PANSS_p</i> : mean ± <i>SD</i>	24.67 ± 4.27	<i>n.s.</i>	<i>n.s.</i>
<i>PANSS_n</i> : mean ± <i>SD</i>	13.43 ± 4.97	<i>n.s.</i>	<i>n.s.</i>
<i>PANSS_g</i> : mean ± <i>SD</i>	36.13 ± 4.17	<i>n.s.</i>	<i>n.s.</i>
<i>PANSS_t</i> : mean ± <i>SD</i>	74.23 ± 8.56	<i>n.s.</i>	<i>n.s.</i>

SD Standard deviation, *n.s.* non-significant, *PANSS* positive and negative symptom scale, *PANSS_p* positive scale score obtained from *PANSS*, *PANSS_n* negative scale score obtained from *PANSS*, *PANSS_g* general psychopathology score obtained from *PANSS*, *PANSS_t*, *PANSS* total score

^a *p* value obtained using the χ^2 test

^b *p* value obtained using the two-tailed two samples *t* test

same as those for the FE-SCZ patients, with the exception that they also had to have no history of mental illnesses and no first-degree relatives with a psychotic disorder according to the non-patient version of SCID. Table 1 lists the demographics of all the subjects in detail. In this study, all the subjects were native Chinese speakers and gave written informed consent in accordance with protocols approved by the Clinical Research Ethics Committee of the 3rd Affiliated Hospital of Sun Yat-sen University.

DTI data and T1-weighted 3D high-resolution brain images were acquired for each subject on a 1.5 T GE MRI scanner located at the 3rd Affiliated Hospital of Sun Yat-sen University (see Supplement for acquisition parameters).

Data preprocessing

The effects of head motion and image distortion caused by eddy currents were corrected by applying an affine alignment to register all other diffusion images to the b_0 images in the original DTI data using the FSL/FDT (FSL 4.1: <http://www.fmrib.ox.ac.uk/fsl>). The corrected DTI data were processed using DTIstudio (Version 2.40, <https://www.dtistudio.org>) to reconstruct streamlines throughout the whole brain, based on the Fiber Assignment by Continuous Tracking (FACT) algorithm (Mori et al. 1999). A streamline was initiated from each voxel and followed the main diffusion direction or the principal eigenvector of each voxel. Tracking was stopped when the fractional

anisotropy (FA) < 0.2 or the angle between the eigenvectors of two consecutive voxels was >45°.

Network construction

An anatomical network representing inter-regional white matter pathways was constructed using diffusion tractography and the automated anatomical labeling atlas (AAL) (Tzourio-Mazoyer et al. 2002), which contains 90 regions of interest (ROIs) in the cortical and subcortical regions (AAL-90). Inter-regional detectable streamline and the streamline counts were defined as the edge and the inter-regional connectivity strength, respectively. In order to reduce the false-positive connections resulted from the noise signal or limitations of the deterministic tracking method, we considered any pair of regions to be anatomically connected if at least three streamlines were located between two regions (Lo et al. 2010; Shu et al. 2011; Brown et al. 2011). This may maximize statistical robustness, minimize the need for arbitrary choices (such as threshold of streamline counts) (Bassett et al. 2011; Ginestet et al. 2011), and ensure the largest size (ninety) of connected component in the anatomical networks observed across all the controls (Shu et al. 2011; Wang et al. 2012). Meanwhile, we also tested the influence of different thresholds of streamline counts on the network analysis. The details of the network construction are described in the Supplement and can also be found in previous publications (Wang et al. 2012; Gong et al. 2009a).

Network analysis

The topological properties of the human brain anatomical networks were analyzed using graph theory. We characterized the global properties of the networks by the following parameters: network strength (S_p), shortest path length (L_p), degree (K_p), global efficiency (E_{glob}), local efficiency (E_{loc}), and small-worldness (σ). In addition, we used nodal efficiency (E_{nod}) and nodal degree (K_i) to describe the nodal properties of the anatomical networks. A region was defined as a hub or pivotal node if its E_{nod} was at least one standard deviation (*SD*) greater than the mean nodal efficiency of the network, i.e., $E_{nod} > \text{mean} + SD$. The definitions of these parameters are presented in the Supplement.

Robustness of brain anatomical networks

Robustness (ρ) represents the network's resilience to either targeted or random attack (Lynall et al. 2010). In a targeted attack, network nodes are removed one by one in descending order of nodal efficiency (E_{nod}), whereas in a random attack, network nodes are randomly removed

independent of their E_{nod} . The detailed procedures for performing a targeted attack and a random attack are described in the Supplement.

Statistical analysis

Nonparametric permutation tests which inherently accounts for multiple comparisons (Nichols and Holmes 2002; Nichols and Hayasaka 2003) were employed to assess the statistical significance of between-group differences for each of the global parameters and each of the nodal parameters for a given node. Briefly, for a given parameter, we first estimated the t value to indicate the between-group difference. Then we randomly assigned the parameter values for all subjects in this study into two groups to re-calculate the t value between the two randomized groups. We repeated the permutation 10,000 times and obtained 10,000 t values. Finally, we determined the significance level of the between-group differences at 95 % of the empirical distribution in a two-tailed test.

A network-based statistic (NBS) approach (Zalesky et al. 2010a) was used to determine any connected subnetwork in which each of inter-regional connections was significantly changed in the FE-SCZ patients compared to the controls. A detailed description of the NBS is described in the Supplement as well as in Zalesky et al. (2010a). In performing the NBS calculations, the primary threshold for each inter-regional connection was set to a t value > 1.68 or $p < 0.05$ (5,000 permutations).

For the global parameters and nodal parameters that showed significant between-group differences, we calculated the Pearson's correlation between these parameters and the clinical variables of the FE-SCZ patients. The clinical variables included the PANSS total score ($PANSS_t$), PANSS positive subscale ($PANSS_p$), PANSS negative subscale ($PANSS_n$), and PANSS general subscale ($PANSS_g$).

Validating the reproducibility

Reproducibility of the anatomical network properties has been extensively studied based on DW-MRI data, such as definitions of node (Bassett et al. 2011; Ginestet et al. 2011; Zalesky et al. 2010b). Here, we construct brain networks by selecting three different definitions of nodes with different thresholds of streamline counts (1–6), and tested the reproducibility of network properties.

Effect of streamline counts intersecting a pair region

In order to evaluate the reproducibility of the obtained topological properties of brain anatomical networks using the threshold of three streamline counts, we also performed

repeated calculations using alternative thresholds ranging from 1 to 6 streamline counts. The network parameters were presented as a function of the threshold of the streamline counts.

Effect of different parcellation schemes

We estimated the reproducibility of our main findings, which were obtained using the AAL-90, by employing two other parcellation schemes, the Harvard-Oxford atlas, which contains 110 ROIs (HOA-110) (Makris et al. 1999; Kennedy et al. 1998) and the high-resolution AAL atlas, which contains 1024 ROIs of equal size (AAL-1024) (Zalesky et al. 2010b).

Cross-validation with a bootstrap approach

The confidence intervals of the network parameters, S_p , L_p , K_p , E_{glob} , E_{loc} , and σ , in the FE-SCZ patients and the controls were estimated using a bootstrap approach with 1,000 randomizations (Pajevic and Bassler 2003). Using sampling with replacement, after randomly drawing an individual from the original sample, the individual was put back before drawing the next one. Each resample, therefore, had the same size as the original sample, i.e., $n = 30$ for the FE-SCZ patients and $n = 34$ for the controls.

Results

Inter-regional anatomical connectivity

Figure 1 demonstrates a single connected subnetwork identified using the NBS method. The subnetwork contains 36 nodes and 40 inter-regional connections (details listed in Table S5 in the Supplement). We noticed that within this subnetwork, the values of all the connections were significantly decreased in the FE-SCZ patients compared to the controls ($p = 0.033$, corrected), and most of the impaired connections in the FE-SCZ patients were between the frontal, parietal, occipital and subcortical regions. Figure 2 shows the Pearson's correlations between the global parameters and the mean value of the edge weights contained in the subnetwork at $p < 0.05$. We found that the extent of the reduction in connectivity strength was positively correlated with degree (K_p , $r = 0.57$, $p = 0.001$) and with global efficiency (E_{glob} , $r = 0.62$, $p = 2.4e-4$) and significantly negatively correlated with shortest path length (L_p , $r = -0.59$, $p = 5.4e-4$) in the FE-SCZ patients.

Global parameters

We tested the small-world properties of the anatomical networks for the FE-SCZ patients and the controls and

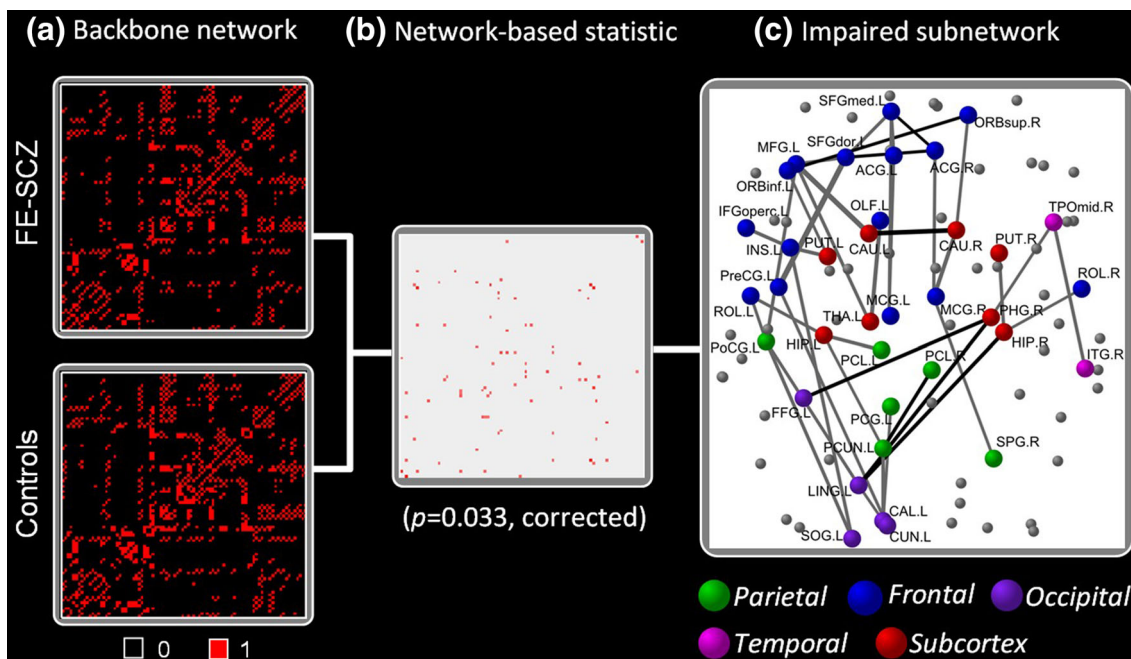


Fig. 1 Significantly changed inter-regional anatomical connections in the medication-naïve, first-episode schizophrenia (FE-SCZ) patients identified using the network-based statistic (NBS) approach. No significantly increased inter-regional connection was detected in the FE-SCZ patients compared to the controls. **a** Detecting significant nonzero connections within each group by performing a nonparametric one-tailed sign test. The number of inter-regional connections was 444 (539) for the patients (controls) determined using a one-

tailed sign test ($p = 0.05$, Bonferroni correction). The sparsity of the anatomical connectivity matrix for the patients (0.1109) was 17.63 % less than for the controls (0.1345). **b** Impaired connections identified using the NBS approach ($p = 0.033$, corrected) for the FE-SCZ patients. **c** Circular plot of the impaired connections. The regions belonging to the frontal, parietal, subcortical, occipital, and temporal regions are color-coded in *blue*, *green*, *red*, *purple*, and *pink*, respectively (For details, see Table S4 in the Supplement)

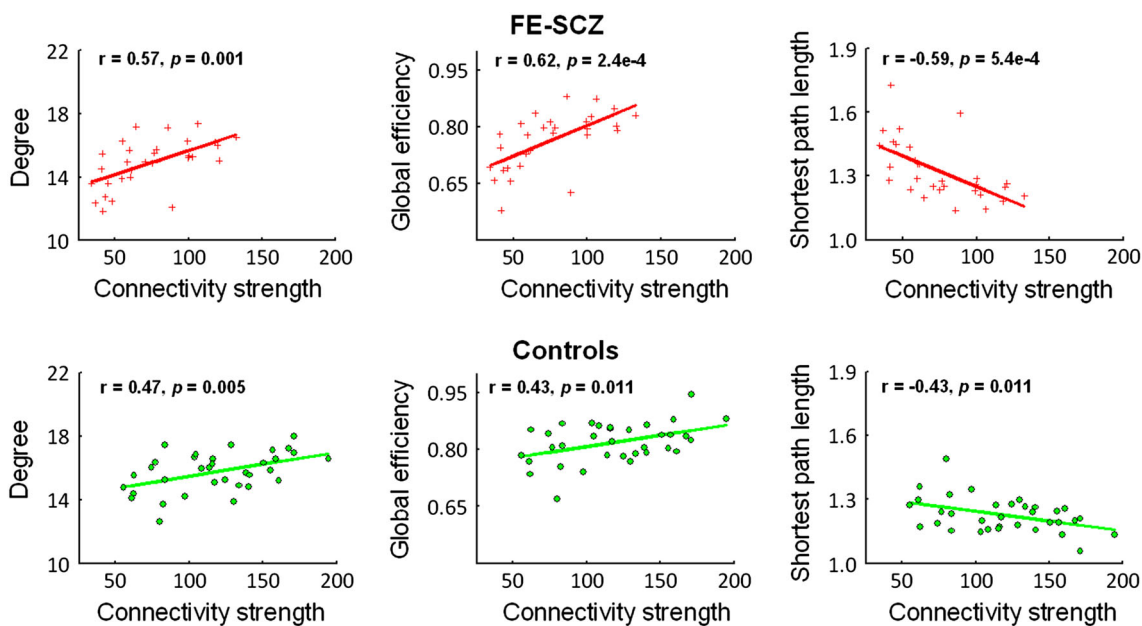


Fig. 2 Scatter plots of the global network parameters (degree, global efficiency, and shortest path length) against the mean inter-regional connectivity strength within the NBS-based network for the

medication-naïve, first-episode schizophrenia (FE-SCZ) patients (*Crosses*) and the controls (*Circles*)

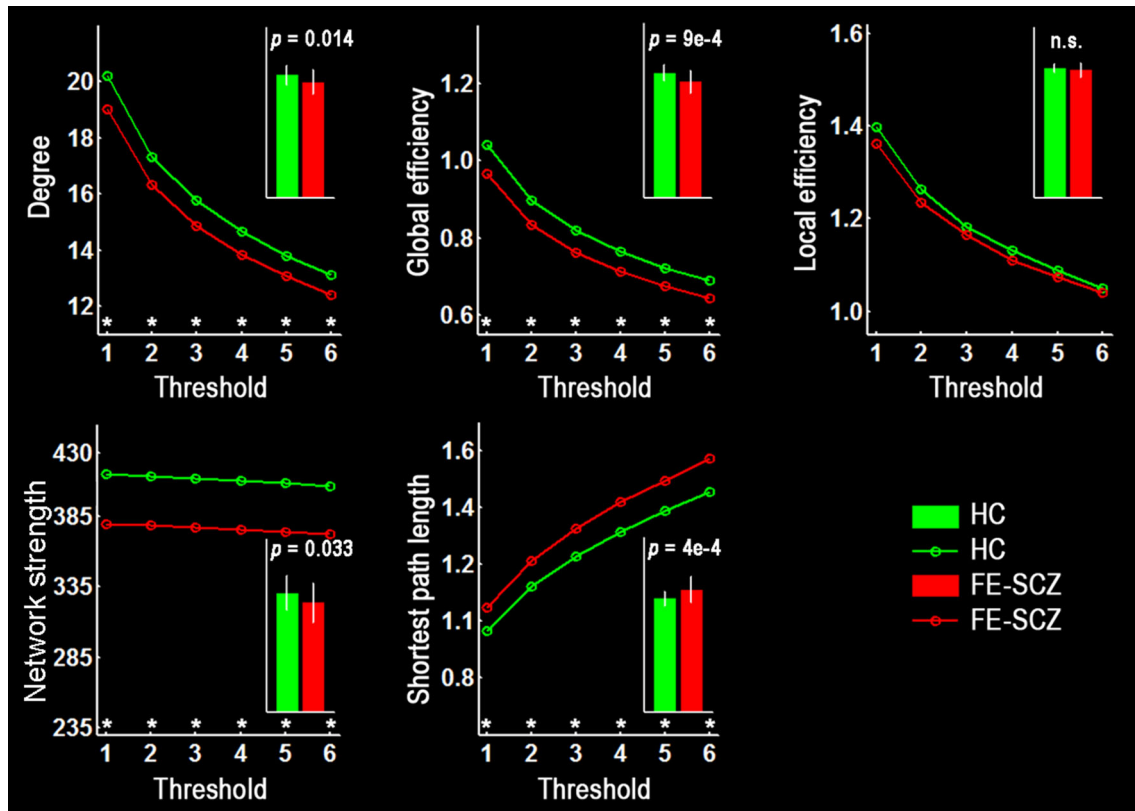


Fig. 3 Global parameters of the brain anatomical networks changing with the selected threshold of streamline counts for the medication-naïve, first-episode schizophrenia (FE-SCZ) patients and the controls (HC). The threshold of the streamline counts ($n = 1, 2, 3, 4, 5,$ and 6) was the minimum number of streamline counts connecting a pair of regions when constructing the networks based on the AAL-90. The FE-SCZ patients showed significant decreases in global efficiency (E_{glob}), degree (K_p), and network strength (S_p) but a significant

increase in shortest path length (L_p) compared to the controls ($p < 0.05$, permutation test). The symbol * indicates $p < 0.05$ for between-group differences. The inserted *bar plot* indicates the between-group comparisons corresponding to a threshold of $n = 3$. The *bar* height represents the mean value and the error bar represents the standard deviation for the given network parameter over all subjects in each group

found $\sigma > 1$ for both of them (Table S2 in the Supplement), which suggests that the anatomical networks of both subject groups possess small-world characteristics. For each subject, we calculated the values of K_p , E_{glob} , E_{loc} , S_p , and L_p for the anatomical network. For both groups, the values of these global parameters changed with the selected threshold (1–6 streamline counts), that is, with the number of streamline counts, as illustrated in Fig. 3. We found that the values of K_p , E_{glob} , E_{loc} , and S_p of the patients were less than those of the controls, whereas the value of L_p of the patients was higher than that of the controls. The inserted bar plot in Fig. 3 illustrates the between-group comparison result when we used a threshold of three streamline counts. In this situation, we found that the patients showed significantly increased L_p ($p = 7e-4$), but significantly decreased E_{glob} ($p = 9e-4$) and K_p ($p = 0.014$) as well as S_p ($p = 0.035$) compared to the controls. No significant between-group difference was detected for the E_{loc} .

Nodal parameters

Table 2 lists all the brain regions showing significant between-group differences, obtained using nonparametric permutation tests ($p < 0.05$, uncorrected), in at least one of the nodal parameters, E_{nod} and K_i . Figure 4a illustrates the locations of these regions. We found they are primarily located in four different systems: the top-down control system, for which we found the right middle frontal gyrus (MFG.R), left insula (INS.L), left anterior cingulate gyrus (ACG.L), right middle cingulate gyrus (MCG.R), left inferior parietal lobule (IPL.L), left precuneus (PCUN.L), and right middle occipital gyrus (MOG.R); the sensorimotor system, for which we found the right supplementary motor area (SMA.R), left postcentral gyrus (PoCG.L), left paracentral lobule (PCL.L), left superior parietal gyrus (SPG.L), and right supramarginal gyrus (SMG.R); and the basal ganglia system, for which we found the bilateral caudate (CAU.L/R), bilateral thalamus (THA.L/R), and left

Table 2 Brain regions showing abnormal nodal parameters (nodal efficiency E_{nod} and nodal degree K_i) of brain anatomical networks in the FE-SCZ patients compared to the healthy controls (HC)

Regions	Location	Nodal efficiency (E_{nod})			Nodal degree (K_i)		
		FE-SCZ	HC	<i>p</i> value	FE-SCZ	HC	<i>p</i> value
Top-down control system							
MFG.R	Frontal	0.90	1.02	0.042	19.90	23.01	0.117
INS.L	Frontal	0.92	0.99	0.035	27.91	28.26	0.638
ACG.L	Frontal	0.59	0.69	0.024	8.29	10.02	0.062
MCG.R	Frontal	1.01	1.09	0.025	28.34	30.45	0.196
IPL.L	Parietal	0.83	0.91	0.034	15.04	16.20	0.348
MOG.R	Occipital	0.65	0.74	0.035	9.06	11.03	0.122
PCUN.L	Parietal	1.08	1.19	0.008	28.71	34.10	0.007
Sensorimotor system							
PoCG.L	Parietal	0.91	1.01	0.028	20.28	23.73	0.072
PCL.L	Parietal	0.57	0.74	0.013	7.17	10.26	0.064
SPG.L	Parietal	1.01	1.12	0.012	21.48	25.84	0.056
SMA.R	Frontal	0.45	0.65	0.020	5.52	7.90	0.140
SMG.R	Parietal	0.70	0.81	0.008	9.08	11.61	0.020
Basal ganglia system							
CAU.R	Basal ganglia	0.62	0.68	0.036	7.78	9.52	0.030
THA.R	Basal ganglia	0.84	0.92	0.035	19.93	20.68	0.637
THA.L	Basal ganglia	0.89	0.98	0.014	21.98	22.63	0.671
CAU.R	Basal ganglia	0.54	0.63	0.011	6.16	8.02	0.030
PUT.L	Basal ganglia	0.66	0.78	5.0e-4	12.27	14.87	0.040
Limbic-visual system							
OLF.L	Frontal	0.39	0.49	0.003	4.24	5.05	0.168
CUN.L	Occipital	0.75	0.84	0.036	12.86	13.56	0.674

The network properties of a given brain region were considered abnormal in the FE-SCZ patients if at least one of the nodal parameters exhibited significant between-group differences ($p < 0.05$, uncorrected) (shown in bold font). These regions were primarily located in the top-down control, sensorimotor, basal ganglia, and limbic-visual systems. The analysis indicated the nodal parameters of these regions in the FE-SCZ patients were uniformly less than those of the controls

putamen (PUT.L). Statistical analyses indicated that the values of nodal parameters for these brain regions were uniformly significantly decreased in the FE-SCZ patients compared to the controls (Fig. 4b).

Hub regions

The hub regions were determined based on the nodal efficiency (E_{nod}). Figure 5 shows the detected hub regions, 13 and 17 hub regions, of the brain anatomical networks for the patients and the controls, respectively (Table S2 in the Supplement). All of the 13 hubs found in the FE-SCZ patients were also detected in the controls. Four additional hubs, the right precentral gyrus (PreCG.R), MFG.L/R, and PoCG.L, were found in the controls but not in the FE-SCZ patients.

Resilience of the brain anatomical networks

The robustness of the brain anatomical networks for the two groups was also investigated. We found that the networks for

the controls demonstrated greater robustness in response to either a random error or a targeted attack than those for the patients (Fig. S1 in the Supplement). Compared to the controls, the network robustness in response to a random attack was significantly decreased in the patients ($p < 0.05$).

Relationship between network parameters and PANSS

We estimated the correlations between the global parameters (S_p , L_p , K_p , and E_{glob}) of the network and the patients' clinical variables ($PANSS_t$, $PANSS_p$, $PANSS_n$ and $PANSS_g$ scores) and also between the mean values of the inter-regional connections within the NBS-based subnetwork and the clinical variables. However, we found no significant correlation between any of these network parameters and any of the clinical variables ($p > 0.05$).

The correlations between the nodal parameters and the clinical variables were tested. We found that the values of E_{nod} for the SMA.R and PoCG.L were significantly negatively correlated not only with $PANSS_t$ but also with

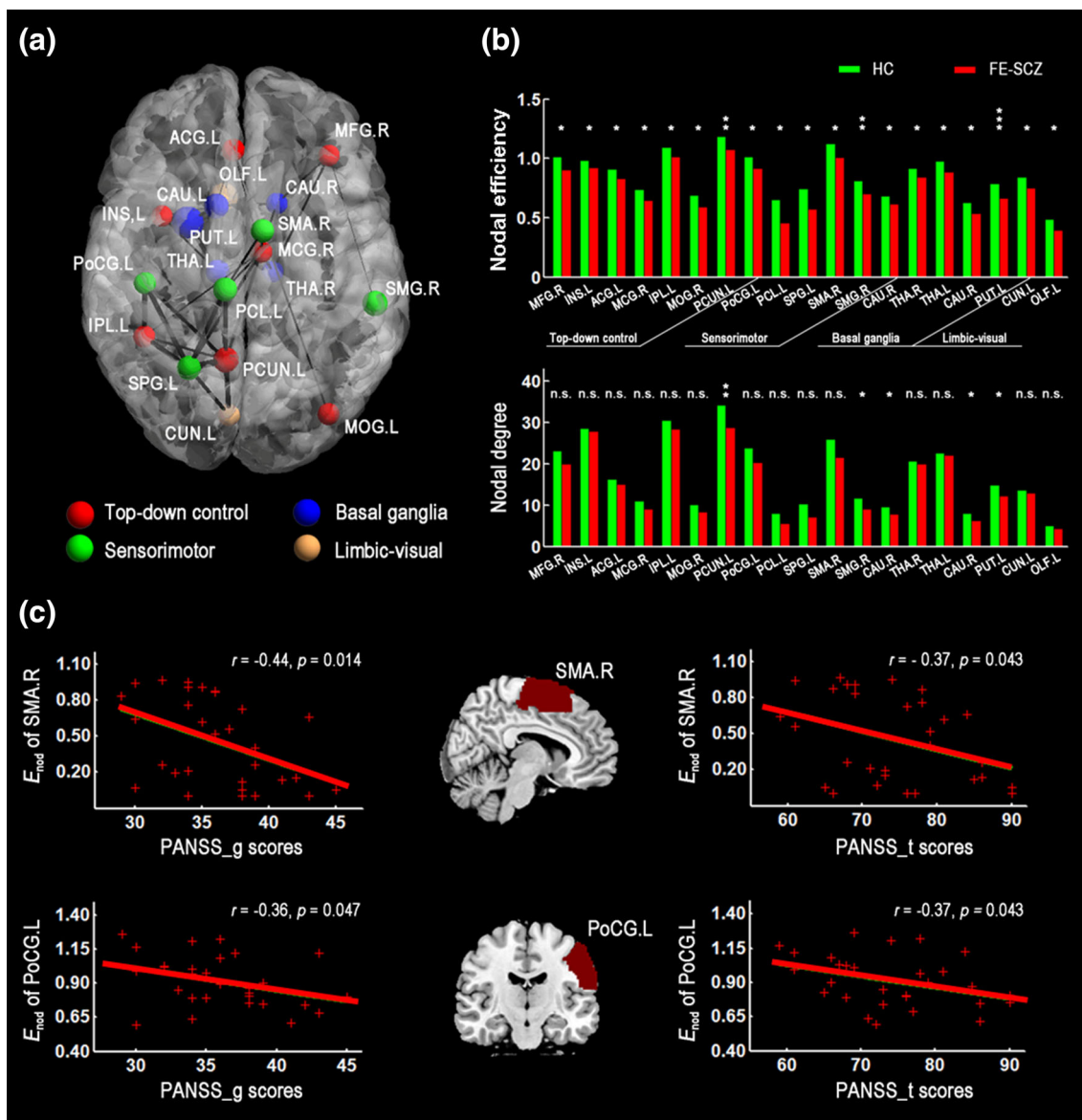


Fig. 4 Brain regions with significantly changed nodal parameters in the medication-naïve, first-episode schizophrenia (FE-SCZ) patients. **a** Distribution of the regions with changed nodal parameters. 19 regions showed significantly decreased, and no region showed significantly increased, nodal parameters at $p < 0.05$ (uncorrected) in the FE-SCZ patients compared to the controls. Nodes color-coded in red, blue, green, and yellow correspond to the top-down control, basal ganglia, sensorimotor, and limbic-visual systems. **b** Comparison of the mean nodal efficiency and degree between the patient group

and the control group for each of these 19 regions. The symbol * stands for $p < 0.05$, ** for $p < 0.01$, *** for $p < 0.001$, and n.s. for non-significant. **c** Correlations between nodal efficiency (E_{nod}) and PANSS_g and between E_{nod} and PANSS_t for the right supplementary motor area (SMA.R) and left postcentral gyrus (PoCG.L) in the patients ($p < 0.05$, corrected). PANSS Positive and Negative symptom scale, PANSS_g general psychopathology score obtained from PANSS, PANSS_t PANSS total score

PANSS_g scores ($p < 0.05$, corrected) (Fig. 4c). In addition, we found the values of E_{nod} for the IPL.L and PCL.L exhibited marginally significant correlations with PANSS_g scores ($0.05 < p < 0.1$) (Fig. S2 in the Supplement).

Reproducibility of the findings

The reproducibility of the network analysis was analyzed using the following strategies. First, we estimated the

confidence interval of the global network parameters (S_p , K_p , E_{glob} , E_{loc} , L_p , and σ) for the AAL-90 using the bootstrap approach. The analysis indicated that the 95 % confidence interval for a given network parameter was distributed closely to the same parameter in the original sample of the patients and controls across 1,000 random sub-samples (Table S4 in the Supplement). Second, to explore the dependence of our results on the choice of threshold, we selected different streamline counts

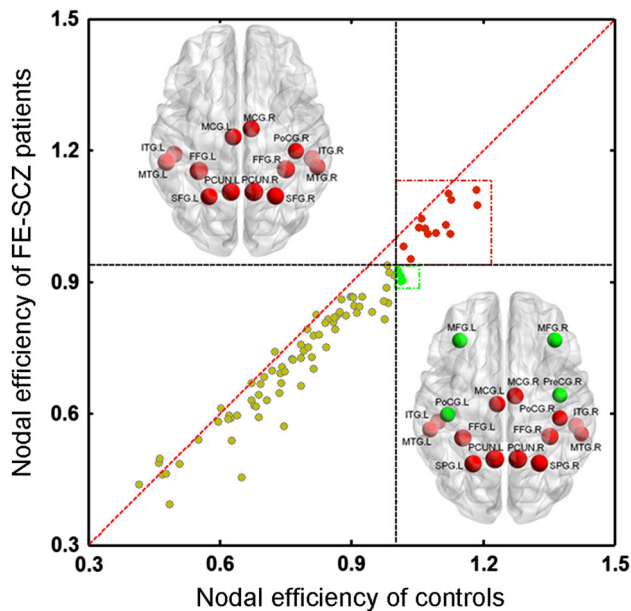


Fig. 5 Correspondence of the nodal efficiency between the anatomical networks of the medication-naïve, first-episode schizophrenia (FE-SCZ) patients and the controls (HC). Using the criterion, $E_{\text{nod}} > \text{mean} + SD$, we determined 13 hubs for the FE-SCZ patients and 17 hubs for the controls. The vertical and horizontal dashed lines correspond to the criterion values of $E_{\text{nod}} = \text{mean} + SD$, which were 0.94 and 1.01 for the patients and the controls, respectively. The circles symbol represents 90 regions of the AAL-90. The circles color-coded in yellow stand for non-hub regions. The circles and the nodes color-coded in red stand for the hubs that occurred in both groups, while the circles and nodes coded in green were for the hubs specific to the controls. The four hubs specific to the controls were the bilateral middle frontal gyrus (MFG.L/R), left postcentral gyrus (PoCG.L), and right precentral gyrus (PreCG.R) (color-coded in green)

thresholds (1–6 streamline counts) to construct brain networks according to the AAL-90. Similar results were consistently observed (Fig. 3 and Table S5 in the Supplement). Third, two other brain parcellation schemes, HOA-110 and AAL-1024, were used to define nodes for constructing brain networks. We found that the direction of the changes in the network parameters (S_p , K_p , E_{glob} , L_p) for these two atlases was same as those for the AAL-90 in the patients compared to the controls (Table 3), although the nodes showing the altered nodal parameters for these two schemes differed from those for the AAL-90 (Figs. S3 and S4 in the Supplement).

Discussion

Using diffusion tractography and graph theory analysis, we compared the FE-SCZ patients to the controls on measures of anatomical connectivity and on network parameters. The NBS-based analysis revealed that white matter integrity was disrupted in the FE-SCZ patients. We found that along

with alterations in the white matter integrity, the global and nodal parameters of the anatomical networks were significantly changed in the FE-SCZ patients. Taken together, these results may indicate that at a macroscale or at the scale of axonal fiber bundles, the dysconnectivity or abnormal connectivity existed in SCZ patients. This may also suggest that the network organization was changed in early phase of the psychosis.

Inter-regional anatomical connectivity

In this study, we found that most of the impaired connections in the FE-SCZ patients were located in the frontal, parietal and occipital regions (Fig. 1c and Table S3 in the Supplement). The results portrayed in Fig. 1c indicated that the frontal regions of the FE-SCZ patients were less connected to the parietal and occipital regions via the cingulum bundle and fronto-occipital fasciculus, and that the low integrity of hemispheric connections through the corpus callosum was also detected. Cingulate dysfunction has been suggested as an aspect of the pathophysiology of SCZ (Benes 1993; Fornito et al. 2009; Glahn et al. 2008; Wilmsmeier et al. 2010). Previous studies detected morphological changes in the cingulum (Seal et al. 2008; Kubicki et al. 2003; Manoach et al. 2007), fronto-occipital fasciculus (Cheung et al. 2008; Nakamura et al. 2012; Lee et al. 2013; Gasparotti et al. 2009), and corpus callosum (Cheung et al. 2008; Walterfang et al. 2008) in SCZ patients. Our findings of aberrant anatomical connectivity between the frontal/parietal and subcortical regions is in line with morphological studies (Ellison-Wright et al. 2008) and DTI studies (Zhang et al. 2010; White et al. 2012a; Rosenberger et al. 2012). For example, Ellison-Wright et al. (2008) performed a meta-analysis of anatomical changes in first-episode SCZ and found that they broadly coincided with a basal ganglia-thalamo-cortical circuit. Zhang et al. (2010) identified abnormal FA in the anterior thalamic radiation/anterior limb of the internal capsule in SCZ patients. In addition, we detected the abnormal anatomical connectivity in temporal regions (ITG.R and TPOMid.R) in the FE-SCZ patients, which is largely compatible with previous DTI studies (Tang et al. 2007; Asami et al. 2013; Quan et al. 2013; Ellison-Wright and Bullmore 2009). Ellison-Wright and Bullmore (2009) performed a meta-analysis study in SCZ patients on DTI data, and found that white matter microstructure in the temporal cortex may be predominantly affected by the disorder in SCZ patients. Asami et al. (2013) found the mean FA of middle longitudinal fascicle (MLF), which connects the ITG and TPOMid, significantly decreased in SCZ patients compared to controls. The MLF is believed to involve in language, high-order auditory association, visuospatial attention, audiovisual integration, and auditory

Table 3 Cross-validation of the main findings of the network properties of brain anatomical networks between the FE-SCZ patients and the healthy controls (HC) over different parcellation schemes

Network parameters	Group	AAL-90		HOA-110		AAL-1024	
		Mean	<i>p</i> value	Mean	<i>p</i> value	Mean	<i>p</i> value
S_p	FE-SCZ	376.95	0.033	281.62	0.015	89.73	0.014
	HC	411.59		309.10		98.12	
E_{glob}	FE-SCZ	0.76	9.0e-4	0.86	4.1e-2	0.32	2.7e-3
	HC	0.82		0.91		0.35	
L_p	FE-SCZ	1.33	4.0e-4	1.17	2.9e-2	3.19	2.9e-3
	HC	1.23		1.11		2.86	
K_p	FE-SCZ	14.87	0.014	16.59	3.3e-2	12.90	3.7e-3
	HC	15.75		17.45		13.92	
E_{loc}	FE-SCZ	1.16	0.192	1.44	0.071	0.77	9.8e-3
	HC	1.18		1.48		0.81	
σ	FE-SCZ	2.60	–	2.58	–	11.83	–
	HC	2.52		2.50		11.72	

AAL-90, Anatomical automatic Labeling atlas with 90 region of interests (ROIs), HOA-110 Harvard–Oxford atlas with 110 ROIs, AAL-1024 high-resolution randomly generated atlas with 1024 ROIs. The shown bold font exhibited network parameters were considered abnormal in FE-SCZ patients if they exhibited significant between-group differences ($p < 0.05$)

spatial information (Makris et al. 2012). Deficits of these functions in the MLF are core features of schizophrenia. Compared with previous studies that used FA to detect aberrant anatomical connectivity in the MLF in SCZ patients, the network analysis adopted here is a more obvious and direct method for detecting changes of brain anatomical connectivity in FE-SCZ patients.

Global parameters

The calculations showed small-worldness ($\sigma > 1$) in the FE-SCZ patients and the controls, which indicated that the anatomical networks for both groups have small-world properties. This result is consistent with previous studies of brain anatomical networks (Gong et al. 2009a, b).

Do the brain parcellation schemes or the threshold of streamline counts affect the direction of the changes in the global network parameters in the patients? We detected significant decreases in degree (K_p) and network strength (S_p) as well as in global efficiency (E_{glob}), but a significant increase in the shortest path length (L_p) in the FE-SCZ patients compared to the controls regardless of which of the brain parcellation schemes (atlases AAL-90, HOA-110 and AAL-1024) was selected (Table 3). In addition, for the AAL-90, the direction of the changes for each of the global parameters (K_p , E_{glob} , E_{loc} , S_p , and L_p) was independent of the choice of threshold of streamline counts (Fig. 3). These results are consistent with several previous studies of brain anatomical networks in SCZ (Table S6 in the Supplement). As suggested by van den Heuvel et al. (2010), the changes in these network parameters may result either from reduced

inter-regional connectivity strength between the cortical and subcortical areas or from longer pathway disconnections. We noticed that the K_p , E_{glob} , and L_p of the FE-SCZ patients were all significantly correlated with the mean connectivity strength within the NBS-based subnetwork (Fig. 2). This may imply that the significantly decreased connectivity strength in the subnetwork contributes to the abnormality of the global topological organization in FE-SCZ patients.

Nodal parameters

In the FE-SCZ patients, we detected significantly decreased nodal parameters in regions of the frontal, parietal, occipital, and basal ganglia. These regions primarily fell into four functional systems: the top–down control, sensorimotor, basal ganglia, and limbic-visual systems.

Top–down control system We found significantly decreased nodal degree and nodal efficiency in the FE-SCZ patients primarily in the top–down control system (ACGL, MCG.R, IPL.L, PCUN.L, MFG.R, INS.L, and MOG.R) (Dosenbach et al. 2007; Zhang et al. 2011) (Table 2; Fig. 4a, b). Previous studies (Barch and Keefe 2010; Bora et al. 2010) indicated that the deficits of cognitive control system are a typical characteristic of SCZ patients. Several studies suggested that in the cingulate cortex (ACG and MCG), gray matter volume was decreased (Wang et al. 2007; Calabrese et al. 2008), functional activity hypo-activated (Adams and David 2007), and WM integrity disrupted (Takei et al. 2009; Ellison-Wright and Bullmore 2009) in SCZ patients compared to controls. Our result of the decreased nodal efficiency in the

frontal (MFG.R and INS.L) are consistent with several previous fMRI studies in SCZ patients (Pujol et al. 2013; Barch and Ceaser 2012). Vercammen et al. (2012) studied 20 SCZ patients and found that the input–output response of the frontal cortex was increased during response inhibition to positive words in SCZ patients. Løberg et al. (2012) reported the decreased activation in the IPL and PCUN in SCZ patients when they attended an auditory dichotic listening task. In addition, our result of decreased nodal efficiency in the MOG in the SCZ-related is largely compatible with several fMRI studies in SCZ patients (White et al. 2012b; Turner et al. 2013; Koeda et al. 2013). Thus, our findings provide structural evidence for the changes that might underlie these functional deficits in FE-SCZ patients.

Sensorimotor system We detected significantly decreased degree and nodal efficiency in the SMA.R, PoCG.L, PCL.L, SPG.L and SMG.R, core components of the sensorimotor system, in the FE-SCZ patients compared to the controls (Table 2; Fig. 4a, b). We also found that in the SMA.R and PoCG.L, the value of E_{nod} correlated negatively with the $PANSS_t$ and $PANSS_g$ scores in the FE-SCZ patients (Fig. 4c). This indicates that the more severe the psychiatric symptoms in FE-SCZ, the lower the values of E_{nod} in the SMA.R and PoCG.L. This result is in line with morphological studies (Heuser et al. 2011; Exner et al. 2006). Exner et al. (2006) found structural abnormality in the left pre-SMA in first-episode SCZ patients, and Heuser et al. (2011) showed that minor motor and sensory deficits were significantly associated with reduced gray matter densities in the PoCG and IPL in first-episode SCZ patients. Taken together, we suggest that the value of E_{nod} in the PoCG and SMA may be useful for detecting the severity of psychiatric symptoms in SCZ.

Basal ganglia system In the FE-SCZ patients, we observed a significantly decreased degree and nodal efficiency in the THA.L/R, CAU.L/R, and PUT.L (Table 2; Fig. 4a, b), which belong to the basal ganglia system (Draganski et al. 2008; Haber 2003). The thalamus, a highly evolved gateway for sensory and motor inputs to the cortex, plays an important role in the cognitive and perceptual disturbances of SCZ patients (Carlsson 1988). Several studies found the thalamic volume of SCZ patients to be significantly smaller than that of the comparison subjects (Gilbert et al. 2001; Adriano et al. 2010; Haijma et al. 2012). We also found decreased nodal efficiency in CAU.L/R and PUT.L in the FE-SCZ patients, which is line with previous studies (Levitt et al. 2013, 2012; Duff et al. 2013; Sorg et al. 2013). Haijma et al. (2012) carried out a brain volume meta-analysis in SCZ based on over 18,000 subjects in 317 studies and found that the reductions of gray matter volume in the caudate nucleus and thalamus were more pronounced in antipsychotic-naïve SCZ patients than in medicated SCZ patients. Taking these previous

studies together, our finding of abnormal nodal metrics in caudate and thalamus provide further evidence that the aberrant basal ganglia system is an intrinsic feature of SCZ patients (Ellison-Wright et al. 2008; Mamah et al. 2008).

Limbic-visual system We found that the nodal efficiency in the CUN.L and OLF.L was significantly decreased in the FE-SCZ patients (Table 2; Fig. 4a, b), indicating deficits of the limbic-visual system. The CUN is believed to have a variety of cognitive functions, including working memory (Bluhm et al. 2011), behavioral engagement (Zhang and Li 2012), monitoring changes of ocular position in response to self-generated eye movements (Law et al. 1998). Actually, Whitford et al. (2012) have suggested that SCZ patients may have abnormalities in monitoring their self-generated eye movements. Our findings of the decreased nodal efficiency in OLF.L in FE-SCZ patients is compatible with a previous study, which suggested the depth of olfactory sulcus may be a static vulnerability marker of SCZ patients (Takahashi et al. 2012).

Topological vulnerability in anatomical networks of FE-SCZ

Dynamic behavior of a network is strongly associated with its fundamental topological organization. The alterations in network parameters would reflect the disruptions in the general performance of the network such as robustness and stability. We found that the FE-SCZ patients' networks were less robust in response to either a random error or a targeted attack compared to the controls. This reduced topological stability might be attributed to altered cerebral organization in the FE-SCZ patients, such as the decreased white matter connectivity. However, several previous studies constructed brain functional networks based on the resting-state fMRI (rsfMRI) data and found increased robustness to targeted and random node removal in SCZ patients (Alexander-Bloch et al. 2010; Lynall et al. 2010). And these studies (Alexander-Bloch et al. 2010; Lynall et al. 2010) detected significantly increased global efficiency in the functional networks in SCZ patients. On the contrary, Zalesky et al. (2011) and Wang et al. (2012) revealed significantly decreased global efficiency in brain anatomical networks derived from DTI data. The inconsistent tendencies of brain network robustness may be caused by the different image modalities (DTI and rsfMRI) or subject heterogeneity. A further study combining resting-state fMRI and DTI data should be used to address these divergences.

Limitations

The following issues need to be further addressed. First, the present study used a suboptimal DTI sequence with 15

diffusion-encoding gradient directions and non-isotropic voxel size in the magnetic field 1.5T. A study (Jones 2004) has shown that at least 20 unique sampling orientations are necessary for a robust estimation of anisotropy, whereas at least 30 unique sampling orientations are required for a robust estimation of tensor orientation and mean diffusivity (Posnansky et al. 2011). To address the potential effects of a suboptimal DTI sequence with 15 diffusion-encoding gradient directions, we repeated the network analysis using different inter-regional connectivity threshold and different brain parcellation schemes, and found that the results showed a high reproducibility across subjects. It suggests that our findings are reliable, although some suboptimal scanning parameters were used here. Using similar scanning sequences, recent studies also reported a high reproducibility of the white matter network properties (Gong et al. 2009a; Shu et al. 2011). Nonetheless, the analysis should be performed on the high angular DTI datasets collected with optimal sequence parameters to further evaluate the reproducibility of our results. Second, we utilized diffusion deterministic tractography to draw white matter tracks for constructing the brain anatomical networks. Previous studies have pointed out that using deterministic tractography as the tracking procedure may result in a loss of the ability to detect crossed fibers (Mori and van Zijl 2002), or the uncertainty of determining fiber orientation is high in regions with crossing, twisting or kissing fiber tracts (Jbabdi and Johansen-Berg 2011). Other methods, such as probabilistic tractograph, may increase the sensitivity of fiber reconstruction. Third, although we found reliable disease-related changes across different parcellation schemes (Table 3) and different connectivity thresholds (Fig. 3), mapping the brain networks appropriately and precisely is a challenging task at the present time (Butts 2009). We still do not know which of the brain parcellation schemes is best for constructing brain anatomical networks. However, just as is discussed above, the impacts of the parcellation schemes on the network properties were consistent across the two subject groups in this study, which indicated that the parcellation schemes may not affect the reproducibility of our results. Fourth, the diffusion gradients (bvecs or B-matrix) introduced by head motion were not corrected (Leemans and Jones 2009) when correcting for subject motion in the DTI data from this study. However, we think that this effect should be small in comparison with other effects (such as the signal dropout effects or the interaction between motion and field inhomogeneity) that we cannot correct. Finally, even though the nonparametric permutation test inherently accounts for multiple comparisons (Nichols and Holmes 2002; Nichols and Hayasaka 2003), the nodal parameters were not corrected with multiple comparisons in this study. Thus, the results should be considered as an exploratory analysis.

In summary, we investigated the topological properties of brain anatomical networks for medication-naïve, first-episode schizophrenia (FE-SCZ) patients, who were free from mediating treatments and who had short illness duration. To the best of our knowledge, this is the first study using diffusion tractograph to show alterations of the brain anatomical networks for FE-SCZ patients. We uniformly detected significantly decreased inter-regional connections and global efficiency as well as degree in the FE-SCZ patients compared to the controls, and the nodal efficiency in the sensorimotor system correlated negatively with the severity of psychosis symptoms in the FE-SCZ patients. Our findings indicate that abnormalities exist in the brain anatomical networks of SCZ patients and suggest that the network organization may be changed in the early stages of the SCZ disease process.

Acknowledgments This work was partly supported by the 3rd Affiliated Hospital of Sun Yat-sen University, the funding of National Natural Science Foundation of China (Grant Numbers: 81071149, 81271548, and 81371535), Natural Science Foundation of Guangdong Province (Grant Numbers: S2012010009027), and Scientific Research Foundation for the Returned Overseas Chinese Scholars (RH), State Education Ministry of China. The authors appreciate the editing assistance of Drs. Rhoda E. and Edmund F. Perozzi. The authors also would like to thank the anonymous reviewers for their constructive comments and suggestions.

Conflict of interest The authors reported no biomedical financial interests or potential of conflicts of interest.

References

- Adams R, David AS (2007) Patterns of anterior cingulate activation in schizophrenia: a selective review. *Neuropsychiatric Dis Treat* 3(1):87–101
- Adriano F, Spoletini I, Caltagirone C, Spalletta G (2010) Updated meta-analyses reveal thalamus volume reduction in patients with first-episode and chronic schizophrenia. *Schizophr Res* 123(1):1–14
- Alexander-Bloch AF, Gogtay N, Meunier D, Birn R, Clasen L, Lalonde F, Lenroot R, Giedd J, Bullmore ET (2010) Disrupted modularity and local connectivity of brain functional networks in childhood-onset schizophrenia. *Front Syst Neurosci* 4:147
- Amador XF, Gorman JM (1998) Psychopathologic domains and insight in schizophrenia. *Psychiatric Clin N Am* 21(1):27–42
- Asami T, Saito Y, Whitford TJ, Makris N, Niznikiewicz M, McCarley RW, Shenton ME, Kubicki M (2013) Abnormalities of middle longitudinal fascicle and disorganization in patients with schizophrenia. *Schizophr Res* 143(2–3):253–259
- Barch DM, Ceaser A (2012) Cognition in schizophrenia: core psychological and neural mechanisms. *Tren Cogn Sci* 16(1):27–34
- Barch DM, Keefe RS (2010) Anticipating DSM-V: opportunities and challenges for cognition and psychosis. *Schizophr Bull* 36(1):43–47
- Bassett DS, Brown JA, Deshpande V, Carlson JM, Grafton ST (2011) Conserved and variable architecture of human white matter connectivity. *Neuroimage* 54(2):1262–1279

- Beasley CL, Dwork AJ, Rosoklija G, Mann JJ, Mancevski B, Jakovski Z, Davceva N, Tait AR, Straus SK, Honer WG (2009) Metabolic abnormalities in fronto-striatal-thalamic white matter tracts in schizophrenia. *Schizophr Res* 109(1):159–166
- Benes FM (1993) Neurobiological investigations in cingulate cortex of schizophrenic brain. *Schizophr Bull* 19(3):537
- Bluhm RL, Clark CR, McFarlane AC, Moores KA, Shaw ME, Lanius RA (2011) Default network connectivity during a working memory task. *Hum Brain Mapp* 32(7):1029–1035
- Bora E, Yücel M, Pantelis C (2010) Cognitive impairment in schizophrenia and affective psychoses: implications for DSM-V criteria and beyond. *Schizophr Bull* 36(1):36–42
- Brown JA, Terashima KH, Burggren AC, Ercoli LM, Miller KJ, Small GW, Bookheimer SY (2011) Brain network local interconnectivity loss in aging APOE-4 allele carriers. *Proc Natl Acad Sci* 108(51):20760–20765
- Butts CT (2009) Revisiting the foundations of network analysis. *Science* 325(5939):414–416
- Calabrese DR, Wang L, Harms MP, Ratnanather JT, Barch DM, Cloninger CR, Thompson PA, Miller MI, Csernansky JG (2008) Cingulate gyrus neuroanatomy in schizophrenia subjects and their non-psychotic siblings. *Schizophr Res* 104(1):61–70
- Camchong J, Lim KO, Sponheim SR, MacDonald AW III (2009) Frontal white matter integrity as an endophenotype for schizophrenia: diffusion tensor imaging in monozygotic twins and patients' nonpsychotic relatives. *Front Hum Neurosci* 3:35
- Carlsson A (1988) The current status of the dopamine hypothesis of schizophrenia. *Neuropsychopharmacology* 1(3):179–186
- Cheung V, Cheung C, McAlonan G, Deng Y, Wong J, Yip L, Tai K, Khong P, Sham P, Chua S (2008) A diffusion tensor imaging study of structural dysconnectivity in never-medicated, first-episode schizophrenia. *Psychol Med* 38(06):877–885
- Cheung V, Chiu C, Law C, Cheung C, Hui C, Chan K, Sham P, Deng M, Tai K, Khong P-L (2011) Positive symptoms and white matter microstructure in never-medicated first episode schizophrenia. *Psychol Med* 41(08):1709–1719
- Dosenbach NU, Fair DA, Miezin FM, Cohen AL, Wenger KK, Dosenbach RA, Fox MD, Snyder AZ, Vincent JL, Raichle ME (2007) Distinct brain networks for adaptive and stable task control in humans. *Proc Natl Acad Sci* 104(26):11073–11078
- Douaud G, Smith S, Jenkinson M, Behrens T, Johansen-Berg H, Vickers J, James S, Voets N, Watkins K, Matthews PM (2007) Anatomically related grey and white matter abnormalities in adolescent-onset schizophrenia. *Brain* 130(9):2375–2386
- Draganski B, Kherif F, Kloppel S, Cook PA, Alexander DC, Parker GJ, Deichmann R, Ashburner J, Frackowiak RS (2008) Evidence for segregated and integrative connectivity patterns in the human Basal Ganglia. *J Neurosci* 28(28):7143–7152
- Duff BJ, Macritchie KA, Moorhead TW, Lawrie SM, Blackwood DH (2013) Human brain imaging studies of DISC1 in schizophrenia, bipolar disorder and depression: a systematic review. *Schizophr Res* 147(1):1–13
- Ellison-Wright I, Bullmore E (2009) Meta-analysis of diffusion tensor imaging studies in schizophrenia. *Schizophr Res* 108(1):3–10
- Ellison-Wright I, Glahn DC, Laird AR, Thelen SM (2008) The anatomy of first-episode and chronic schizophrenia: an anatomical likelihood estimation meta-analysis. *Amer J Psychiatry* 165(8):1015
- Exner C, Weniger G, Schmidt-Samoa C, Irle E (2006) Reduced size of the pre-supplementary motor cortex and impaired motor sequence learning in first-episode schizophrenia. *Schizophr Res* 84(2–3):386–396
- Filippi M, Canu E, Gasparotti R, Agosta F, Valsecchi P, Lodoli G, Galluzzo A, Comi G, Sacchetti E (2013) Patterns of brain structural changes in first-contact, antipsychotic drug-naïve patients with schizophrenia. *Amer J Neuroradiol*. doi:10.3174/ajnr.A3583
- Fornito A, Yücel M, Dean B, Wood SJ, Pantelis C (2009) Anatomical abnormalities of the anterior cingulate cortex in schizophrenia: bridging the gap between neuroimaging and neuropathology. *Schizophr Bull* 35(5):973–993
- Friedman J, Tang C, Carpenter D, Buchsbaum M, Schmeidler J, Flanagan L, Golembos S, Kanellopoulou I, Ng J, Hof P (2008) Diffusion tensor imaging findings in first-episode and chronic schizophrenia patients. *Amer J Psychiatry* 165(8):1024–1032
- Friston KJ (1999) Schizophrenia and the disconnection hypothesis. *Acta Psychiatr Scand Suppl* 395:68–79
- Gasparotti R, Valsecchi P, Carletti F, Galluzzo A, Liserre R, Cesana B, Sacchetti E (2009) Reduced fractional anisotropy of corpus callosum in first-contact, antipsychotic drug-naïve patients with schizophrenia. *Schizophr Res* 108(1):41–48
- Gilbert AR, Rosenberg DR, Harenski K, Spencer S, Sweeney JA, Keshavan MS (2001) Thalamic volumes in patients with first-episode schizophrenia. *Amer J Psychiatry* 158(4):618–624
- Ginestet CE, Nichols TE, Bullmore ET, Simmons A (2011) Brain network analysis: separating cost from topology using cost-integration. *PLoS One* 6(7):e21570
- Glahn DC, Laird AR, Ellison-Wright I, Thelen SM, Robinson JL, Lancaster JL, Bullmore E, Fox PT (2008) Meta-analysis of gray matter anomalies in schizophrenia: application of anatomic likelihood estimation and network analysis. *Biol Psychiatry* 64(9):774–781
- Gong G, He Y, Concha L, Lebel C, Gross DW, Evans AC, Beaulieu C (2009a) Mapping anatomical connectivity patterns of human cerebral cortex using in vivo diffusion tensor imaging tractography. *Cereb Cortex* 19(3):524–536
- Gong G, Rosa-Neto P, Carbonell F, Chen ZJ, He Y, Evans AC (2009b) Age- and gender-related differences in the cortical anatomical network. *J Neurosci* 29(50):15684–15693
- Guo W, Liu F, Liu Z, Gao K, Xiao C, Chen H, Zhao J (2012) Right lateralized white matter abnormalities in first-episode, drug-naïve paranoid schizophrenia. *Neurosci Lett* 531(1):5–9
- Haber SN (2003) The primate basal ganglia: parallel and integrative networks. *J Chem Neuroanat* 26(4):317–330
- Hagmann P, Kurrant M, Gigandet X, Thiran P, Wedeen VJ, Meuli R, Thiran JP (2007) Mapping human whole-brain structural networks with diffusion MRI. *PLoS One* 2(7):e597
- Hajima SV, Van Haren N, Cahn W, Koolschijn PCM, Pol HEH, Kahn RS (2012) Brain volumes in schizophrenia: a meta-analysis in over 18 000 subjects. *Schizophr Bull* 39(5):1129–1138
- Heitmiller DR, Nopoulos PC, Andreasen NC (2004) Changes in caudate volume after exposure to atypical neuroleptics in patients with schizophrenia may be sex-dependent. *Schizophr Res* 66(2):137–142
- Heuser M, Thomann PA, Essig M, Bachmann S, Schroder J (2011) Neurological signs and morphological cerebral changes in schizophrenia: an analysis of NSS subscales in patients with first episode psychosis. *Psychiatry Res* 192(2):69–76
- Jbabdi S, Johansen-Berg H (2011) Tractography: where do we go from here? *Brain Connect* 1(3):169–183
- Jones DK (2004) The effect of gradient sampling schemes on measures derived from diffusion tensor MRI: a Monte Carlo study†. *Magn Reson Med* 51(4):807–815
- Kennedy D, Lange N, Makris N, Bates J, Meyer J, Caviness V (1998) Gyri of the human neocortex: an MRI-based analysis of volume and variance. *Cereb Cortex* 8(4):372–384
- Koeda M, Takahashi H, Matsuura M, Asai K, Okubo Y (2013) Cerebral responses to vocal attractiveness and auditory hallucinations in schizophrenia: a functional MRI study. *Front Human Neurosci* 7:221

- Kong X, Ouyang X, Tao H, Liu H, Li L, Zhao J, Xue Z, Wang F, Jiang S, Shan B (2011) Complementary diffusion tensor imaging study of the corpus callosum in patients with first-episode and chronic schizophrenia. *J Psychiatry Neurosci* 36(2):120
- Kubicki M, Westin C-F, Nestor PG, Wible CG, Frumin M, Maier SE, Kikinis R, Jolesz FA, McCarley RW, Shenton ME (2003) Cingulate fasciculus integrity disruption in schizophrenia: a magnetic resonance diffusion tensor imaging study. *Biol Psychiatry* 54(11):1171–1180
- Kunimatsu N, Aoki S, Kunimatsu A, Abe O, Yamada H, Masutani Y, Kasai K, Yamasue H, Ohtomo K (2012) Tract-specific analysis of white matter integrity disruption in schizophrenia. *Psychiatry Res* 201(2):136–143
- Law I, Svarer C, Rostrup E, Paulson OB (1998) Parieto-occipital cortex activation during self-generated eye movements in the dark. *Brain* 121(11):2189–2200
- Lee S-H, Kubicki M, Asami T, Seidman LJ, Goldstein JM, Mesholam-Gately RI, McCarley RW, Shenton ME (2013) Extensive white matter abnormalities in patients with first-episode schizophrenia: a diffusion tensor imaging (DTI) study. *Schizophr Res* 143(2–3):231–238
- Leemans A, Jones DK (2009) The B-matrix must be rotated when correcting for subject motion in DTI data. *Magn Reson Med* 61(6):1336–1349
- Levitt JJ, Alvarado JL, Nestor PG, Rosow L, Pelavin PE, McCarley RW, Kubicki M, Shenton ME (2012) Fractional anisotropy and radial diffusivity: diffusion measures of white matter abnormalities in the anterior limb of the internal capsule in schizophrenia. *Schizophr Res* 136(1):55–62
- Levitt JJ, Rosow LK, Nestor PG, Pelavin PE, Swisher TM, McCarley RW, Shenton ME (2013) A volumetric MRI study of limbic, associative and sensorimotor striatal subregions in schizophrenia. *Schizophr Res* 145(1–3):11–19
- Lo C-Y, Wang P-N, Chou K-H, Wang J, He Y, Lin C-P (2010) Diffusion tensor tractography reveals abnormal topological organization in structural cortical networks in Alzheimer's disease. *J Neurosci* 30(50):16876–16885
- Løberg E-M, Nygård M, Berle JØ, Johnsen E, Kroken RA, Jørgensen HA, Hugdahl K (2012) An fMRI study of neuronal activation in schizophrenia patients with and without previous cannabis use. *Front Psychiatry* 3:94
- Lynall M-E, Bassett DS, Kerwin R, McKenna PJ, Kitzbichler M, Muller U, Bullmore E (2010) Functional connectivity and brain networks in schizophrenia. *J Neurosci* 30(28):9477–9487
- Makris N, Meyer JW, Bates JF, Yeterian EH, Kennedy DN, Caviness VS (1999) MRI-based topographic parcellation of human cerebral white matter and nuclei: II. Rationale and applications with systematics of cerebral connectivity. *Neuroimage* 9(1):18–45
- Makris N, Preti M, Asami T, Pelavin P, Campbell B, Papadimitriou G, Kaiser J, Baselli G, Westin C, Shenton M (2012) Human middle longitudinal fascicle: variations in patterns of anatomical connections. *Brain Struct Funct* 218(4):951–968
- Mamah D, Harms MP, Wang L, Barch D, Thompson P, Kim J, Miller MI, Csernansky JG (2008) Basal ganglia shape abnormalities in the unaffected siblings of schizophrenia patients. *Biol Psychiatry* 64(2):111–120
- Manoach DS, Ketwaroo GA, Polli FE, Thakkar KN, Barton JJ, Goff DC, Fischl B, Vangel M, Tuch DS (2007) Reduced microstructural integrity of the white matter underlying anterior cingulate cortex is associated with increased saccadic latency in schizophrenia. *Neuroimage* 37(2):599–610
- Mori S, van Zijl PC (2002) Fiber tracking: principles and strategies: a technical review. *NMR Biomed* 15(7–8):468–480
- Mori S, Crain BJ, Chacko VP, van Zijl PC (1999) Three-dimensional tracking of axonal projections in the brain by magnetic resonance imaging. *Ann Neurol* 45(2):265–269
- Nakamura K, Kawasaki Y, Takahashi T, Furuichi A, Noguchi K, Seto H, Suzuki M (2012) Reduced white matter fractional anisotropy and clinical symptoms in schizophrenia: a voxel-based diffusion tensor imaging study. *Psychiatry Res* 202(3):233–238
- Navari S, Dazzan P (2009) Do antipsychotic drugs affect brain structure? A systematic and critical review of MRI findings. *Psychol Med* 39(11):1763
- Nichols T, Hayasaka S (2003) Controlling the family-wise error rate in functional neuroimaging: a comparative review. *Stat Meth Med Res* 12(5):419–446
- Nichols TE, Holmes AP (2002) Nonparametric permutation tests for functional neuroimaging: a primer with examples. *Hum Brain Mapp* 15(1):1–25
- Pajevic S, Bassar PJ (2003) Parametric and non-parametric statistical analysis of DT-MRI data. *J Magn Reson* 161(1):1–14
- Posnansky O, Kupriyanova Y, Shah NJ (2011) On the problem of gradient calibration in diffusion weighted imaging. *Int J Imag Syst Tech* 21(3):271–279
- Pujol N, Penadés R, Rametti G, Catalán R, Vidal-Piñero D, Palacios E, Bargallo N, Bernardo M, Junqué C (2013) Inferior frontal and insular cortical thinning is related to dysfunctional brain activation/deactivation during working memory task in schizophrenic patients. *Psychiatry Res* 214(2):94–101
- Quan M, Lee S-H, Kubicki M, Kikinis Z, Rathi Y, Seidman LJ, Mesholam-Gately RI, Goldstein JM, McCarley RW, Shenton ME (2013) White matter tract abnormalities between rostral middle frontal gyrus, inferior frontal gyrus and striatum in first-episode schizophrenia. *Schizophr Res* 145(1–3):1–10
- Rosenberger G, Kubicki M, Nestor PG, Connor E, Bushell GB, Markant D, Niznikiewicz M, Westin C-F, Kikinis R, Saykin JA (2008) Age-related deficits in fronto-temporal connections in schizophrenia: a diffusion tensor imaging study. *Schizophr Res* 102(1):181–188
- Rosenberger G, Nestor PG, Oh JS, Levitt JJ, Kindlerman G, Bouix S, Fitzsimmons J, Niznikiewicz M, Westin C-F, Kikinis R (2012) Anterior limb of the internal capsule in schizophrenia: a diffusion tensor tractography study. *Brain Imag Behav* 6(3):417–425
- Schlösser RG, Nenadic I, Wagner G, Güllmar D, von Consbruch K, Köhler S, Schultz CC, Koch K, Fitzek C, Matthews PM (2007) White matter abnormalities and brain activation in schizophrenia: a combined DTI and fMRI study. *Schizophr Res* 89(1):1–11
- Seal ML, Yücel M, Fornito A, Wood SJ, Harrison BJ, Walterfang M, Pell GS, Pantelis C (2008) Abnormal white matter microstructure in schizophrenia: a voxel-wise analysis of axial and radial diffusivity. *Schizophr Res* 101(1):106–110
- Shu N, Liu Y, Li K, Duan Y, Wang J, Yu C, Dong H, Ye J, He Y (2011) Diffusion tensor tractography reveals disrupted topological efficiency in white matter structural networks in multiple sclerosis. *Cereb Cortex* 21(11):2565–2577
- Sorg C, Manoliu A, Neufang S, Myers N, Peters H, Schwertthöffer D, Scherr M, Mühlau M, Zimmer C, Drzezga A (2013) Increased intrinsic brain activity in the striatum reflects symptom dimensions in schizophrenia. *Schizophr Bull* 39(2):387–395
- Takahashi T, Nakamura Y, Nakamura K, Ikeda E, Furuichi A, Kido M, Kawasaki Y, Noguchi K, Seto H, Suzuki M (2012) Altered depth of the olfactory sulcus in first-episode schizophrenia. *Prog Neuropsychopharmacol Biol Psychiatry* 40:167–172
- Takei K, Yamasue H, Abe O, Yamada H, Inoue H, Suga M, Muroi M, Sasaki H, Aoki S, Kasai K (2009) Structural disruption of the dorsal cingulum bundle is associated with impaired Stroop performance in patients with schizophrenia. *Schizophr Res* 114(1):119–127
- Tang CY, Friedman J, Shungu D, Chang L, Ernst T, Stewart D, Hajianpour A, Carpenter D, Ng J, Mao X (2007) Correlations between diffusion tensor imaging (DTI) and magnetic resonance

- spectroscopy (1H MRS) in schizophrenic patients and normal controls. *BMC Psychiatry* 7(1):25
- Turner JA, Damaraju E, Van Erp TG, Mathalon DH, Ford JM, Voyvodic J, Mueller BA, Belger A, Bustillo J, McEwen S (2013) A multi-site resting state fMRI study on the amplitude of low frequency fluctuations in schizophrenia. *Front Neurosci* 7:1
- Tzourio-Mazoyer N, Landeau B, Papathanassiou D, Crivello F, Etard O, Delcroix N, Mazoyer B, Joliot M (2002) Automated anatomical labeling of activations in SPM using a macroscopic anatomical parcellation of the MNI MRI single-subject brain. *NeuroImage* 15(1):273–289
- van den Heuvel MP, Mandl RC, Stam CJ, Kahn RS, Pol HEH (2010) Aberrant frontal and temporal complex network structure in schizophrenia: a graph theoretical analysis. *J Neurosci* 30(47):15915–15926
- Vercammen A, Morris R, Green MJ, Lenroot R, Kulkarni J, Carr VJ, Weickert CS, Weickert TW (2012) Reduced neural activity of the prefrontal cognitive control circuitry during response inhibition to negative words in people with schizophrenia. *J Psychiatry Neurosci* 37(6):379
- von Knorring L, Lindstrom E (1992) The Swedish version of the positive and negative syndrome scale (PANSS) for schizophrenia. Construct validity and interrater reliability. *Acta Psychiatr Scand* 86(6):463–468
- Walterfang M, Yung A, Wood AG, Reutens DC, Phillips L, Wood SJ, Chen J, Velakoulis D, McGorry PD, Pantelis C (2008) Corpus callosum shape alterations in individuals prior to the onset of psychosis. *Schizophr Res* 103(1):1–10
- Wang L, Hosakere M, Trein JC, Miller A, Ratnanather JT, Barch DM, Thompson PA, Qiu A, Gado MH, Miller MI (2007) Abnormalities of cingulate gyrus neuroanatomy in schizophrenia. *Schizophr Res* 93(1):66–78
- Wang Q, Su T-P, Zhou Y, Chou K-H, Chen I-Y, Jiang T, Lin C-P (2012) Anatomical insights into disrupted small-world networks in schizophrenia. *Neuroimage* 59(2):1085–1093
- Wen W, He Y, Sachdev P (2011) Structural brain networks and neuropsychiatric disorders. *Curr Opin Psychiatry* 24(3):219–225
- White T, Ehrlich S, Ho B-C, Manoach DS, Caprihan A, Schulz SC, Andreasen NC, Gollub RL, Calhoun VD, Magnotta VA (2012a) Spatial characteristics of white matter abnormalities in Schizophrenia. *Schizophr Bull* 39(5):1077–1086
- White T, Moeller S, Schmidt M, Pardo JV, Olman C (2012b) Evidence for intact local connectivity but disrupted regional function in the occipital lobe in children and adolescents with schizophrenia. *Hum Brain Mapp* 33(8):1803–1811
- Whitford TJ, Wood SJ, Yung A, Cocchi L, Berger G, Shenton ME, Kubicki M, Phillips L, Velakoulis D, Yolken RH (2012) Structural abnormalities in the cuneus associated with herpes simplex virus (type 1) infection in people at ultra high risk of developing psychosis. *Schizophr Res* 135(1):175–180
- Wilmsmeier A, Ohrmann P, Suslow T, Siegmund A, Koelkebeck K, Rothermundt M, Kugel H, Arolt V, Bauer J, Pedersen A (2010) Neural correlates of set-shifting: decomposing executive functions in schizophrenia. *J Psychiatry Neurosci* 35(5):321
- Xia M, He Y (2011) Magnetic resonance imaging and graph theoretical analysis of complex brain networks in neuropsychiatric disorders. *Brain Connect* 1(5):349–365
- Zalesky A, Fornito A, Bullmore ET (2010a) Network-based statistic: identifying differences in brain networks. *Neuroimage* 53(4):1197–1207
- Zalesky A, Fornito A, Harding IH, Cocchi L, Yücel M, Pantelis C, Bullmore ET (2010b) Whole-brain anatomical networks: does the choice of nodes matter? *Neuroimage* 50(3):970
- Zalesky A, Fornito A, Seal ML, Cocchi L, Westin C-F, Bullmore ET, Egan GF, Pantelis C (2011) Disrupted axonal fiber connectivity in schizophrenia. *Biol Psychiatry* 69(1):80–89
- Zhang S, CsR Li (2012) Functional networks for cognitive control in a stop signal task: independent component analysis. *Hum Brain Mapp* 33(1):89–104
- Zhang X, Stein EA, Hong LE (2010) Smoking and schizophrenia independently and additively reduce white matter integrity between striatum and frontal cortex. *Biol Psychiatry* 68(7):674–677
- Zhang T, Wang J, Yang Y, Wu Q, Li B, Chen L, Yue Q, Tang H, Yan C, Lui S (2011) Abnormal small-world architecture of top-down control networks in obsessive-compulsive disorder. *J Psychiatry Neurosci* 36(1):23